

## MISR observations of Etna volcanic plumes

S. Scollo,<sup>1</sup> R. A. Kahn,<sup>2</sup> D. L. Nelson,<sup>3</sup> M. Coltelli,<sup>1</sup> D. J. Diner,<sup>4</sup>  
M. J. Garay,<sup>4</sup> and V. J. Realmuto<sup>4</sup>

Received 26 July 2011; revised 2 February 2012; accepted 3 February 2012; published 27 March 2012.

[1] In the last twelve years, Mt. Etna, located in eastern Sicily, has produced a great number of explosive eruptions. Volcanic plumes have risen to several km above sea level and created problems for aviation and the communities living near the volcano. A reduction of hazards may be accomplished using remote sensing techniques to evaluate important features of volcanic plumes. Since 2000, the Multiangle Imaging SpectroRadiometer (MISR) on board NASA's Terra spacecraft has been extensively used to study aerosol dispersal and to extract the three-dimensional structure of plumes coming from anthropogenic or natural sources, including volcanoes. In the present work, MISR data from several explosive events occurring at Etna are analyzed using a program named MINX (MISR Interactive eXplorer). MINX uses stereo matching techniques to evaluate the height of the volcanic aerosol with a precision of a few hundred meters, and extracts aerosol properties from the MISR Standard products. We analyzed twenty volcanic plumes produced during the 2000, 2001, 2002–03, 2006 and 2008 Etna eruptions, finding that volcanic aerosol dispersal and column height obtained by this analysis is in good agreement with ground-based observations. MISR aerosol type retrievals: (1) clearly distinguish volcanic plumes that are sulphate and/or water vapor dominated from ash-dominated ones; (2) detect even low concentrations of volcanic ash in the atmosphere; (3) demonstrate that sulphate and/or water vapor dominated plumes consist of smaller-sized particles compared to ash plumes. This work highlights the potential of MISR to detect important volcanic plume characteristics that can be used to constrain the eruption source parameters in volcanic ash dispersion models. Further, the possibility of discriminating sulphate and/or water vapor dominated plumes from ash-dominated ones is important to better understand the atmospheric impact of these plumes.

**Citation:** Scollo, S., R. A. Kahn, D. L. Nelson, M. Coltelli, D. J. Diner, M. J. Garay, and V. J. Realmuto (2012), MISR observations of Etna volcanic plumes, *J. Geophys. Res.*, *117*, D06210, doi:10.1029/2011JD016625.

### 1. Introduction

[2] During the last twelve years, Mt. Etna (37.734°N, 15.004°E), in eastern Sicily, has been very active. The summit craters have produced several explosive events, and others have occurred from fractures opened up on the volcano flanks. As an example, at the end of October 2002 an eruptive fissure opened on the upper southern flank of the volcano between 2850 and 2600 m a.s.l., producing continuous explosive activity for almost three months [e.g., Andronico *et al.*, 2005]. This eruption severely impacted the local population around Etna, and affected civil aviation,

mainly because the International Airport of Catania is located only 30 km from the vent, near the main direction of the predominant winds [Scollo, 2006; Barsotti *et al.*, 2010]. To limit risk and reduce economic loss, the Istituto Nazionale di Geofisica e Vulcanologia, Osservatorio Etneo (INGV-OE) has undertaken a study over the past five years aimed at defining precisely the areas that are most vulnerable to volcanic ash interference [Scollo *et al.*, 2009].

[3] Using the experience of past crises, we believe this objective can be reached only through the combined use of different observation systems, ranging from ground-based instruments to satellites, coupled with numerical simulations of the phenomena. Field data allow reconstructing and constraining the main characteristics of explosive activity (e.g., ash volume). In addition, remote sensing measurements from satellites and aircraft can furnish detailed information on volcanic ash dispersal. Such measurements are obtained from the Moderate Resolution Imaging Spectroradiometer (MODIS) [e.g., Corradini *et al.*, 2008], from the Spinning Enhanced Visible and InfraRed Imager (SEVIRI) [e.g., Corradini *et al.*, 2009], from the Advanced Spaceborne

<sup>1</sup>Istituto Nazionale di Geofisica e Vulcanologia, Osservatorio Etneo, Sezione di Catania, Catania, Italy.

<sup>2</sup>Atmospheres Laboratory, NASA Goddard Space Flight Center, Greenbelt, Maryland, USA.

<sup>3</sup>Raytheon Company, Pasadena, California, USA.

<sup>4</sup>Jet Propulsion Laboratory, California Institute of Technology, Pasadena, California, USA.

**Table 1.** Main Specifications of the MISR Instrument

	Specifications
Mission life	possibly until 2018
Instrument mass	148 kg
Global coverage time	Every 9 days, with repeat coverage between 2 and 9 days depending on latitude
Cross-track swath width	380 km common overlap of all 9 cameras
View angles	0, 26.1, 45.6, 60.0, and 70.5 degrees
Radiometric accuracy	3% absolute at maximum signal
Spectral Coverage	4 spectral bands centered on 446, 558, 672, and 867 nm
Spatial resolution	275 m in all bands of the nadir camera and in the red bands of the off-nadir cameras, 1.1 km for the other 24 channels

Thermal Emission and Reflectance radiometer (ASTER) [e.g., *Pugnaghi et al.*, 2006], and also from the Multiangle Imaging SpectroRadiometer (MISR) [e.g., *Scollo et al.*, 2010]. During an emergency, all these data provide valuable complementary information that can be used to verify the forecasts of volcanic ash dispersal models and improve their accuracy.

[4] The MISR sensor on board NASA's Terra spacecraft [*Diner et al.*, 1998] has been used extensively since 2000 to study aerosol dispersal and to extract the three-dimensional structure of plumes coming from anthropogenic or natural sources [e.g., *Stenchikov et al.*, 2006; *Nelson et al.*, 2008; *Fromm et al.*, 2008; *Val Martin et al.*, 2010; *Tosca et al.*, 2011]. The main MISR sensor specifications are reported in Table 1. MISR contains nine cameras pointed at fixed angles in the plane of the satellite ground track; one camera points in the nadir direction, and the others are arranged symmetrically at 26.1°, 45.6°, 60.0°, and 70.5° degrees forward and aft of the nadir direction. Each camera measures scene radiance in four different spectral bands centered at 446, 558, 672, and 867 nm. The suite of multispectral and multiangle measurements provided by MISR allows estimation of plume heights and wind vectors through stereoscopic techniques and provide constraints on aerosol properties from radiometric retrievals [*Kahn et al.*, 2007]. *Scollo et al.* [2010] studied the plumes generated by two eruptions of Etna using MISR observations. The authors reconstructed the three-dimensional shape of the 2001 and 2002 Etna volcanic plumes by combining MISR data and numerical simulations. MISR was also able to retrieve the volcanic plume produced during the Eyjafjallajökull eruption in 2010 for about 600 km (373 miles) downwind (<http://mISR.jpl.nasa.gov>). The considerable economic impact of the Iceland eruption, which shut down air traffic over much of Europe, has motivated the scientific community to improve our understanding of volcanic plume dispersal.

[5] MISR observes the entire planet about once per week, with the coverage frequency increasing toward the poles. The coverage is sufficient to capture many important volcanic events, especially those lasting from days-to-weeks but not phenomena that vary day-to-day or hour-to-hour;

one consequence of the lack of near real-time observations is that MISR can only supplement other, more frequent, observations (e.g., from geostationary instruments).

[6] In this paper, we present an analysis of MISR data for several explosive events that occurred at Etna during the last twelve years. We briefly describe the eruptions which were observed by MISR in section 2. Estimates of plume height and dispersal derived from the MISR data are shown and these results compared with ground-based observations collected during the INGV-OE monitoring activities, as well as with MODIS data collected during the MISR transit. We then interpret the aerosol properties derived from MISR data in the context of eruption activity in section 3. Finally, the potential of MISR to detect important volcanic plume characteristics is discussed in section 4.

## 2. Etna Eruptions

### 2.1. The 2000 Lava Fountains

[7] The first explosive episode occurred on the morning of 26 January and was followed by more than sixty episodes at the South East Crater (SEC) between January and August [*Alparone et al.*, 2003]. These events showed a common evolution: an initial resumption of activity characterized by strombolian explosions, a gradual increase in intensity and frequency of the explosions leading to lava fountain events lasting from a few minutes to hours, and a return to strombolian activity [*Alparone et al.*, 2003; *Behncke et al.*, 2006].

[8] MISR acquired data for the 23 May and 1 June 2000 events. The 23 May and 1 June 2000 paroxysms were the 57th and 59th, respectively, in the year 2000 sequence (Table 2). On 23 May, at about 0300 UTC, a volcanic plume rose up to several km and lasted for about twenty minutes. The 1 June episode was one of the most powerful of the entire 2000 sequence. At 0814 UTC explosive activity at the SEC increased, reaching a climax at 0827 UTC and ending at 0833 UTC. The tephra fallout covered the SE flank of the volcano [*Alparone et al.*, 2007].

### 2.2. The 2001 Flank Eruption

[9] The 2001 eruption produced a complex system of fractures and lava flows from different volcanic vents, as well as different styles of explosive activity [*Calvari et al.*, 2001; *Calvari and Pinkerton*, 2004]. The explosive activity originated from two pit craters at an elevation of 2550 m a.s.l. Phreatomagmatic explosions occurred during the first days of the eruption, between 19 and 24 July, followed by strombolian and Hawaiian style explosions, and then by vulcanian explosions that continued until 6 August [*Scollo et al.*, 2007; *Taddeucci et al.*, 2002]. Volcanic plumes on 20, 22, and 29 July (Table 2) were captured by MISR.

### 2.3. The 2002–03 Flank Eruption

[10] The 2002–03 Etna eruption, which took place between 26 October 2002 and 28 January 2003, was one of the most powerful to occur in the last three centuries. A north-south, 1 km-long eruptive fissure opened on the upper southern flank and mainly produced fire fountains, while a north-south, 340 m-long eruptive fissure on the northern flank chiefly produced lava flows. Due to the long duration of this event, MISR acquired data over volcanic plumes on

**Table 2.** Characteristics of Tephra Fallout and Observations of Column Heights for Those Etna Eruptions Retrieved by MISR

Etna Eruptions	Characteristics of Tephra Fallout and Observations of Column Height
23 May 2000	Lapilli fallout occurred on the ENE flanks of Etna but volcanic ash also fell in Fornazzo, Sant'Alfio and Giarre, located on SE volcano flanks.
01 Jun 2000	Volcanic ash fallout on the SE flanks of the volcano and affected Catania city; the eruption column reached 5 km a.s.l.
20 Jul 2001	Phreatomagmatic explosions formed a dilute ash plume of 3–3.5 km a.s.l. in the NE direction.
22 Jul 2001	Tephra fallout occurred in the SE sector and eruption column reached 3.5–4 km a.s.l.
29 Jul 2001	Strombolian activity forming a diluted plume.
27 Oct 2002	Heavy tephra fallout on the S flanks reaching the town of Ragusa about 100 km from the vent. A fairly sustained column reached 6 km a.s.l.
29 Oct 2002	Tephra fallout occurred on the SE sector of the volcano between Nicolosi and Catania and a fairly sustained and pulsating column rose up to 5.8 km a.s.l.
05 Nov 2002	Tephra fallout to the NE and pulsating activity which formed a volcanic plume of 5.5 km a.s.l. Cloudy weather conditions.
07 Nov 2002	Tephra fallout at Zafferana and Milo, in the E sector of volcano and a fairly sustained and pulsating activity formed a column of 5 km above the vent.
14 Nov 2002	Lava fountaining and pulsating activity produced a plume reaching only 3.5 km a.s.l. Tephra fallout on NW sector. Cloudy weather conditions.
23 Nov 2002	Light ash emission toward the SE sector of the volcano due to strombolian activity.
07 Dec 2002	Light fallout on SE flanks of the volcano with fine ash reaching Siracusa's town about 70 km from the vent. The column reached 4.5 km a.s.l. Cloudy weather conditions.
23 Dec 2002	Eruption column of 4.5 km a.s.l. Cloudy weather conditions.
30 Dec 2002	Volcanic plume dispersal in the SE sector of the volcano and a dilute and pulsating column height reaching 3.5 km a.s.l.
08 Jan 2003	Decline of explosive activity without the presence of a sustained eruption column.
15 Jan 2003	Decline of explosive activity without the presence of a sustained eruption column.
29 Sept 2006	Ash emission associated with explosions at the SEC; volcanic ash reached only some hundreds of meters above the vent and was dispersed toward the E.
16 Nov 2006	Light fallout on the NE sector of the volcano from the SEC and column height reaching 3.5 km a.s.l.
25 Nov 2006	High degassing with extremely reduced presence of volcanic ash.
13 May 2008	Volcanic plume was dispersed toward the NE. Cloudy weather conditions.

eleven occasions (Table 2). On 27 October, Etna showed fairly sustained and composite volcanic plumes [Andronico *et al.*, 2008]. On 23 November the activity was strombolian and the plume contained a very low concentration of volcanic ash. After 23 December, explosive activity decreased and the volcanic plume never exceeded 3.5 km a.s.l., whereas the effusive activity ceased completely on 28 January [Andronico *et al.*, 2005].

#### 2.4. The 2006 Summit Eruptions

[11] During 2006, the eruptive activity began from the SEC on the evening of 14 July, lasted ten days and was mainly characterized by lava emission and strombolian activities

[Neri *et al.*, 2006]. The activity resumed on 31 August, as a lava effusion and more forceful explosive paroxysmal events occurred [Behncke *et al.*, 2009]. Good MISR observations were obtained on 29 September and on 16 and 25 November (Table 2). In particular, on 29 September INGV-OE volcanologists observed ash emission events during field surveys. However, the fallout affected only the northern and western higher flanks of the volcano, whereas the finest ash was dispersed toward the east. The most complex activity took place on 16 November, involving lava flows, ash dispersal, and the formation of pyroclastic density currents [Behncke *et al.*, 2009; Norini *et al.*, 2009]. The explosive activity occurred between 0530 and 1530 UTC and produced a thin tephra deposit [Andronico *et al.*, 2009a]. Another powerful event occurred on 24 November from the SEC starting at 0219 UTC and ceasing at about 1530 UTC. Observations carried out by the volcanologist on duty during field surveys on 25 November, when MISR crossed Etna, reported high degassing from the SEC with extremely reduced volcanic ash emission.

#### 2.5. The 2008 Etna Activity

[12] Etna became active again on 10 May 2008, when a new vent opened at the eastern base of the SEC at 1400 UTC and ended at about 1800 UTC of the same day [Bonaccorso *et al.*, 2011]. The explosive and effusive activity resumed after three days, but observations of the eruptive phenomena were difficult to carry out during this event due to poor weather conditions. A volcanic plume formed around 0930 UTC and dispersed toward the northeast. The activity was detected by MISR on 13 May (Table 2), and ended on 14 May.

### 3. MISR Retrievals

#### 3.1. The MINX Software

[13] MISR plume elevation data analysis was carried out using the MISR Interactive eXplorer (MINX) software [Nelson *et al.*, 2008]. MINX is an open source application and is available free of charge through the Open Channel Foundation (<http://www.openchannelsoftware.com/projects/MINX>). MINX allows users to visualize and analyze smoke, volcanic ash and dust plumes, and to determine the spatial distribution of plume-top heights based on MISR multiangle data. Its strength in the analysis of volcanic plumes lies in the ability to precisely retrieve cloud top heights and winds. MINX is an interactive computer program based on stereo matching [Moroney *et al.*, 2002; Muller *et al.*, 2002], which is strictly a geometric technique, and consequently the height estimates are not sensitive to radiometric calibration uncertainties [Marchand *et al.*, 2010] or the emissivity of the plume material. In MINX, the user identifies a plume outline and the direction of plume motion. Stereo matching and forward modeling are then automatically performed on 1.1 km red-band (672 nm) pixel centers within the plume outline to retrieve heights and winds. MINX is able to match images at sub-pixel resolution by fitting a bi-cubic interpolation function to the matrix of correlation coefficients derived during matching, and by averaging three or more height/wind solutions from different camera pairs.

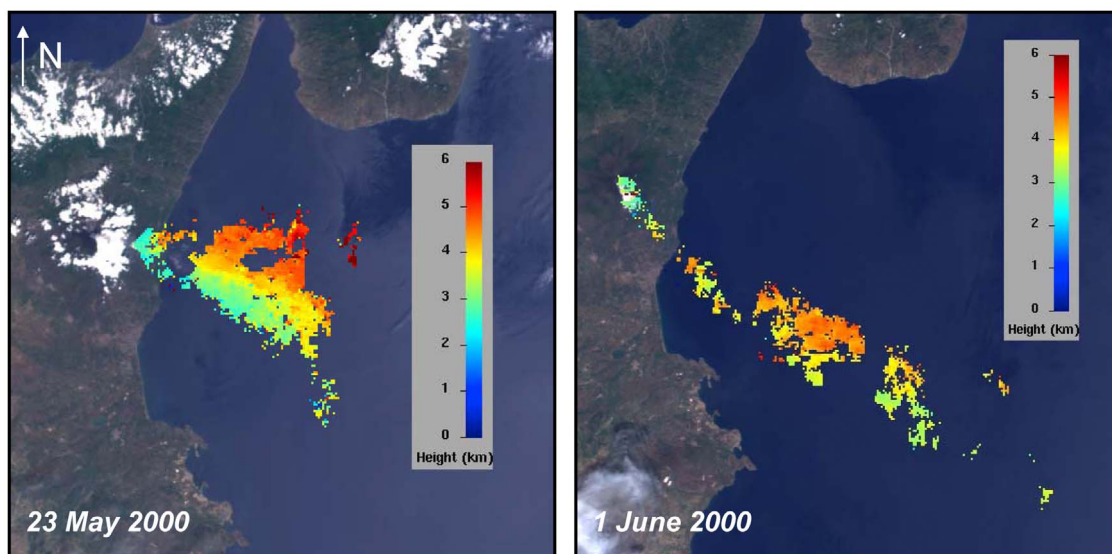
[14] Retrieval quality is diminished if the direction of plume motion is nearly parallel to the along-track direction

**Table 3.** Date and Time of MISR Retrieval, Orbit, Path, and Block, and Main Axes of the Plume Dispersal and Height Obtained by the MINX Software

Etna Eruptions	MISR Data	Median Column Height and Plume Direction
23 May 2000	10:08 UTC, Orbit 2287, path 188, block 60	4.0 km; SE
01 Jun 2000	10:02 UTC, Orbit 2418, path 187, block 48	4.1 km; SE
20 Jul 2001	10:07 UTC Orbit 8447, path 189, block 60	2.8 km; NE
22 Jul 2001	09:07 UTC, Orbit 8476, path 187, block 60	4.8 km; SE
29 Jul 2001	10:01 UTC, Orbit 8578, path 188, block 60	3.6 km; SE
27 Oct 2002	10:00 UTC, Orbit 15204, path 189, block 61	4.1 km; S
29 Oct 2002	09:48 UTC, Orbit 15233, path 187, block 60	7.1 km; SE
05 Nov 2002	09:54 UTC, Orbit 15335, path 188, block 60	3.6 km; NE
07 Nov 2002	09:41 UTC, Orbit 15364, path 186, block 60	4.2 km; E
14 Nov 2002	09:47 UTC, Orbit 15466, path 187, block 60	6.9 km; NW
23 Nov 2002	09:42 UTC, Orbit 15597, path 186, block 60	4.2 km; SE
07 Dec 2002	09:54 UTC, Orbit 15801, path 188, block 60	8.2 km; E
23 Dec 2002	09:54 UTC, Orbit 16034, path 188, block 60	3.9 km; SE
30 Dec 2002	10:04 UTC, Orbit 16136, path 189, block 60	3.7 km; SE
08 Jan 2003	09:54 UTC, Orbit 16267, path 188, block 60	< 3 km; NE
15 Jan 2003	10:00 UTC, Orbit 16369, path 189, block 60	< 3.5 km; NW
29 Sept 2006	09:52 UTC, Orbit 36072, path 188, block 60	3.2 km; E
16 Nov 2006	09:52 UTC, Orbit 36771, path 188, block 60	3.4 km; N; NE
25 Nov 2006	09:46 UTC, Orbit 36902, path 187, block 60	2.8 km; SE
13 May 2008	09:53 UTC, Orbit 44693, path 188, block 60	9.2 km; NE

of the spacecraft motion, if the view of the plume is contaminated by under-lying or over-lying clouds in several cameras (especially the nadir camera), or when plume optical thickness is low over bright backgrounds. For instance, if the optical depth of the aerosol is low enough that the surface is visible through the aerosol, and if the surface has features that render it optically inhomogeneous (e.g., patterns are visible in terrain over land or in sun glint over water), then the pattern matcher will see a combination of aerosol and surface features, and will obtain a poor retrieval, or none at all. Hence, a very low optical depth aerosol over a uniform, dark water background may return good heights, whereas a moderate optical depth aerosol over bright,

variable terrain may return no retrievals. Furthermore, when there is strong vertical motion of aerosols near the vent, or strong turbulence that changes the shape of plume features from camera-to-camera, MINX may not be able to retrieve heights. Due to these multiple factors, no fixed lower limit on optical depth can be specified that uniquely determines whether heights can be retrieved. Consequently, we consider the mean uncertainty in the MINX plume top-heights to be about  $\pm 0.5$  km, equal to MISR's theoretical accuracy [Moroney *et al.*, 2002; Naud *et al.*, 2005]. MINX also extracts data from the MISR Standard aerosol product [Martonchik *et al.*, 2009; Kahn *et al.*, 2010]: aerosol optical depth (AOD) estimates (i.e., the extinction coefficient

**Figure 1.** MISR wind-corrected heights mapped over the corresponding MISR true-color, nadir-view imagery for 23 May and 1 June 2000.

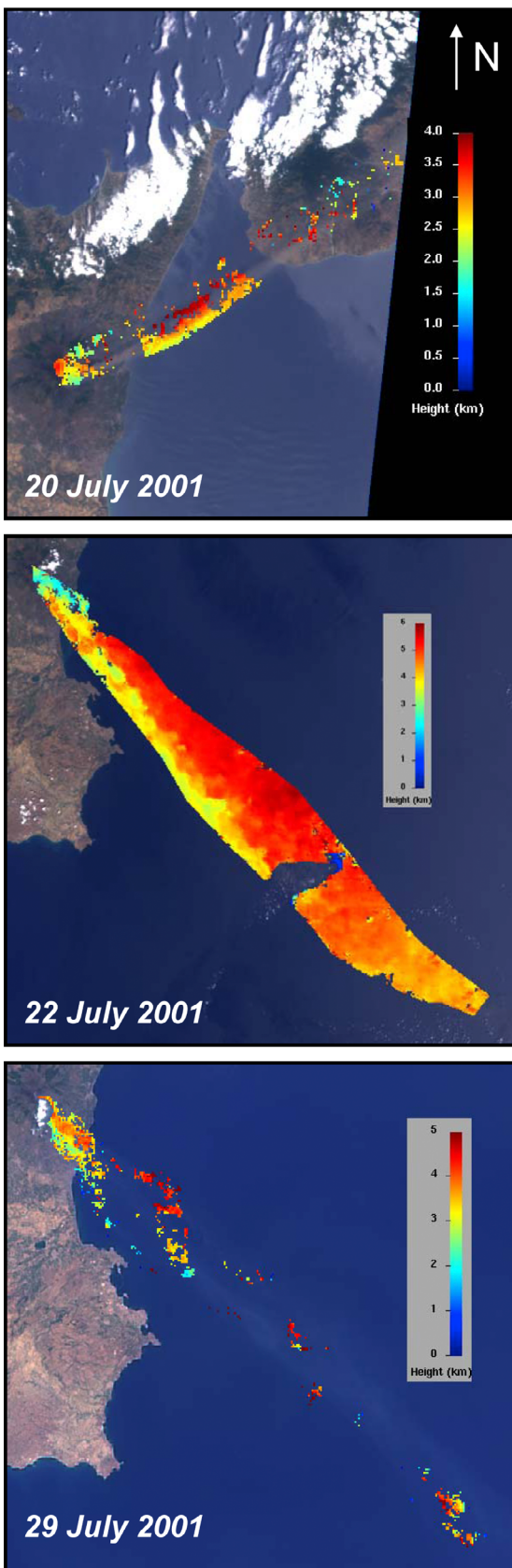


**Figure 2.** MISR wind-corrected heights on 20, 22, and 29 July 2001, superimposed on the corresponding nadir-view imagery.

integrated over a vertical column from the Earth's surface to the top of the atmosphere), the fraction of the MISR-retrieved green band AOD values attributed to spherical particles, as well as the green-band AOD fraction of particles with small size ( $<0.35 \mu\text{m}$ ), medium size (between  $0.35 \mu\text{m}$  and  $0.7 \mu\text{m}$ ), and large size ( $>0.7 \mu\text{m}$ ). We note that the MISR spectral range makes the observations sensitive to the microphysical properties of aerosol with a diameter  $< \sim 2.5 \mu\text{m}$ , though the retrieved AOD accounts for particles of all sizes, and analyses must take this into account when interpreting plume observations.

### 3.2. Plume Dispersal and Height

[15] Table 3 shows dates, times, orbits, paths, and blocks of the cases when MISR detected Etna volcanic plumes, together with the median plume height obtained by MINX and the main plume direction. Figure 1 contains the stereoscopic wind-corrected heights for the 23 May and 1 June 2000 plumes, which were dispersed in the SE direction.

[16] Figure 2 shows the stereoscopic wind-corrected heights for the plumes of 20, 22, and 29 July 2001. The plumes were dispersed toward the NE on 20 July and toward the SE on 22 and 29 July. Lower plume heights were detected on 20 and 29 July, whereas a higher plume height, related to more intense explosive activity ( $\sim 5 \text{ km}$ ), was detected for 22 July (Table 3), in agreement with *Scollo et al.* [2007].

[17] Figure 3 shows the MINX stereoscopic wind-corrected heights retrieved on 27 and 29 October, 23 November, 23 and 30 December 2002. These plumes were dispersed in the S and SE directions. Volcanic aerosol detected on January 2003 was below 3 km (Table 3), confirming that explosive activity dramatically decreased after 30 December 2002 [*Andronico et al.*, 2008].

[18] Figure 4 shows stereoscopic wind-corrected height maps for the plumes of 29 September, 16 and 25 November 2006, and 13 May 2008, which were dispersed over the E, N and NE, SE and NE flanks of the volcano, respectively. The plumes of 25 November followed the orography of Etna, and the height of the ash emission on 29 September did not exceed  $\sim 3.5 \text{ km}$  (Table 3). On 16 November the median value of the column height as retrieved by MINX was 3.5 km. Finally, mainly due to cloud cover, volcanic aerosol was detected only in few pixels over the NE flank of the volcano on 13 May. The height of this aerosol is between 8 and 11 km, and it is similar to the 8 km heights estimated for the plume of 10 May 2008 [*Bonaccorso et al.*, 2011].

[19] Figure 5 shows the plume heights retrieved by MINX compared with ground-based observations (Table 2). We note that the volcanic ash plume produced during Strombolian activity on 29 July 2001 and 23 November 2002 did not exceed 0.5 km above the vent. In this plot we do not include the activity of 23 May 2000 and 13 May 2008, since no ground-observations of column heights were available; neither do we include events in 2003 and most events in 2006, due to their low intensity. For Etna, ground-based observations of column height are usually obtained from the analysis of images and videos captured from different points of view. *Scollo et al.* [2008] suggested that the uncertainty in this method is about 20%. This means that for our data, the column height uncertainty from ground-based observations could range between about  $\pm 0.5$  and  $\pm 1.2 \text{ km}$ .

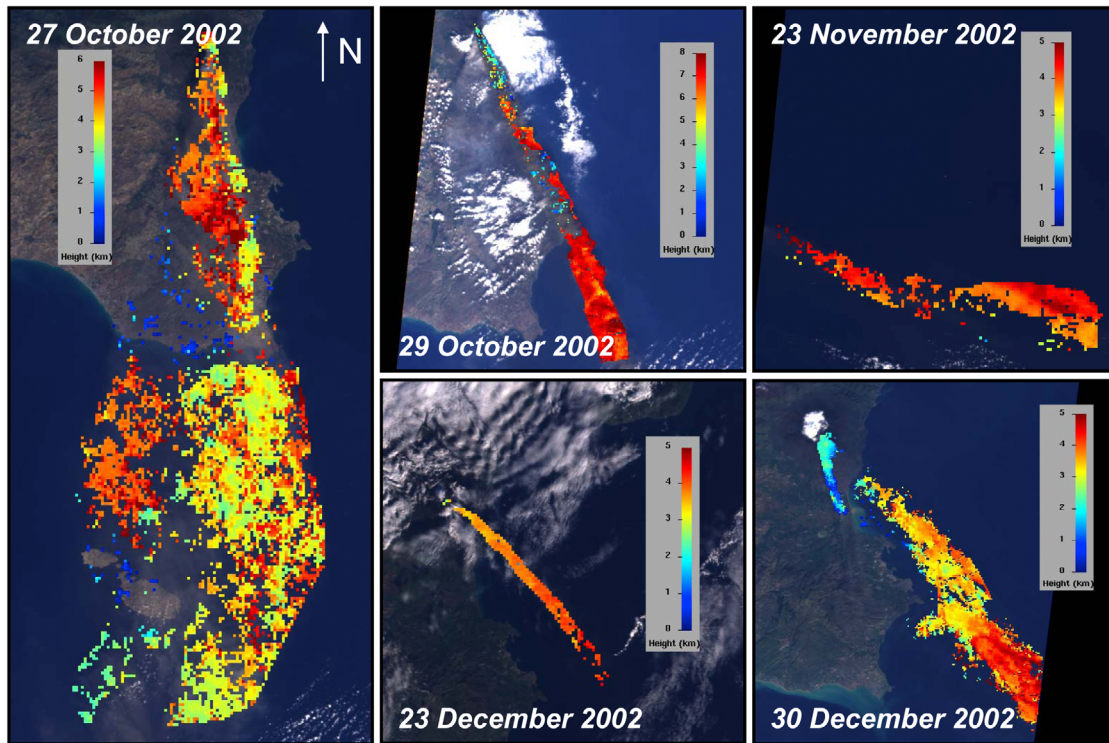


**Figure 3.** MISR wind-corrected heights retrieved on 27 and 29 October, 23 November, 23 and 30 December 2002, superimposed on the corresponding nadir-view imagery.

Furthermore, we note that in those cases when MISR overpasses of Etna and the ground-based observations did not coincide, height discrepancies are expected to increase, especially for those eruptions having high temporal variability.

[20] Field observations and MINX plume-height estimates were in agreement for ten of fourteen events; we found significant differences for four events, all in 2002: 27 October, 5 and 14 November, and 7 December. However, for 27 October 2002, the heights are mainly between 5 and 5.5 km at about 50 km from the vent and stay constant, within 3–4 km, for 150 to 250 km downwind [Scollo *et al.*, 2010]. Hence, if we consider that the ground-based observations estimate column height near the vent in this case as well, the MINX retrieval is in agreement with ground-based observations. For the other three days the weather was cloudy, which can affect both the MISR and ground-based results. In summary, although MISR stereo heights can be difficult to interpret when multilayered clouds are present [Moroney *et al.*, 2002], we find very good agreement between ground-based observations and MINX plume height and dispersal, provided the conditions are not too cloudy.

[21] Figure 6 shows MINX wind-corrected heights as a function of distance from the vent, for volcanic plumes having different eruptive features (Table 2). On 29 October 2002, MINX measured volcanic aerosols between 6 and 8 km a.s.l. as well as aerosols that followed the orography. This may be related to lava descending the north flanks of the volcano and reaching forests. On 23 November 2002 only a portion of the plume farther than 120 km from the

volcanic vent was retrieved, whereas on 29 September 2006 the plume maintained a relatively uniform height of around 3 km. Finally, although the weather was cloudy on 13 May 2008, MINX retrieved heights for aerosols that are clearly volcanic in origin at around 9 km altitude.

### 3.3. Volcanic Aerosol Properties

[22] Table 4 shows volcanic aerosol properties from the MISR Version 22 Standard aerosol product. To obtain good particle property constraints, a component should contribute at least 20% to the total AOD, and total AOD should exceed about 0.15 or 0.2 [Kahn *et al.*, 2010]. For these events, we evaluated the range and mean of AOD values in the green band, the range and mean of MISR-retrieved green band AOD values attributed to spherical particles, and the green band AOD fraction of particles having small, medium, and large size. Our AOD estimates range between 0.03 and 0.58. These results are consistent with optical depth values measured with a Sun photometer at Etna in 1999, which ranged between 0.1 and 0.8 at similar wavelengths, for the 9, 10, and 17 July activity [Watson and Oppenheimer, 2001] and by MODIS on 28, 29, and 30 October 2002 [Corradini *et al.*, 2011]. However, these comparisons are only qualitative, because the observations were not carried out at the same time as the MISR measurements. Consequently, we also compared MISR AOD with the MODIS AOD maps (downloaded from <http://ladsweb.nascom.nasa.gov/data/search.html>). Comparisons were possible for 27 October, 23 November, and 30 December 2002, and for these days, MODIS AOD values (Figure 7) are consistent with MISR.

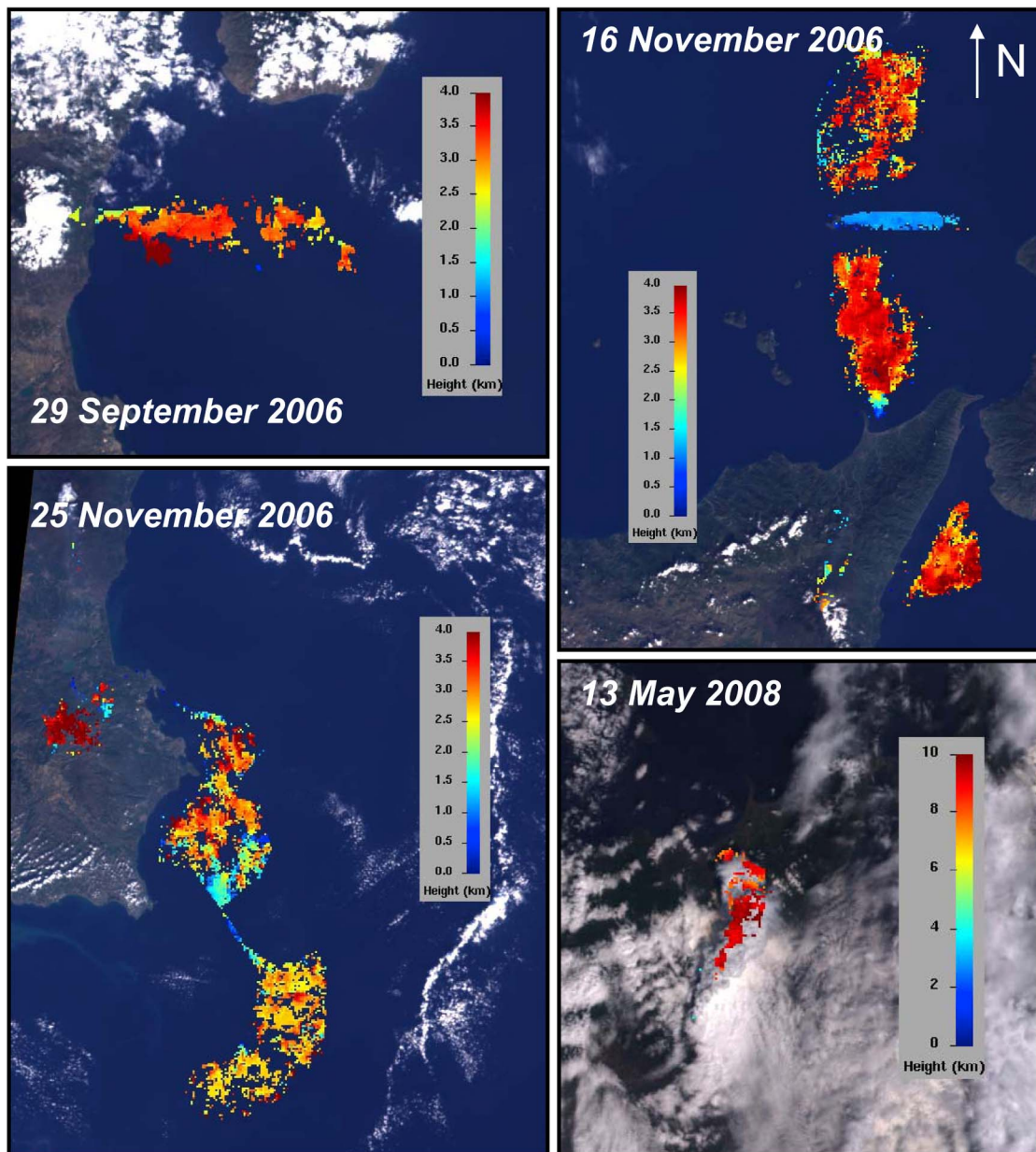


**Figure 4.** MISR wind-corrected heights on 29 September, 16 and 25 November 2006, and 13 May 2008, superimposed on the corresponding nadir-view imagery. Blue points on 16 November 2006 indicate volcanic aerosol coming from Stromboli volcano.

[23] Volcanic ash is highly irregular in shape and consequently the spherical particle AOD fraction is expected to differ from 1. Plumes with a low value of Mean AOD Sph. contain a greater percentage of irregular particles (volcanic ash in our case), whereas plumes with high value of Mean AOD Sph. are characterized by a greater proportion of spherical particles. We found seven cases in which the mean value of Mean AOD Sph. was  $> 0.8$  (Table 4). On 29 July 2001 and 23 November 2002, Etna produced Strombolian activity (Table 2). During this type of activity larger particles usually fall near the volcanic vent, while a low concentration of fine volcanic ash may be present in the atmosphere forming a very diluted plume. The MISR particle type

observations also suggest that the plume was composed mainly of sulphate and/or water vapor components released from the volcano, or was produced from chemical conversion of emitted gases such as  $\text{SO}_2$ . For 8 January 2003, the spherical particle AOD fraction was between 0.8 and 1 (Table 4), in agreement with the end of intense explosive activity reported by *Andronico et al.* [2008] on 30 December 2002. The MISR overpass on 29 September 2006 (0952 UTC) coincided with an ash emission event at 0947 UTC from the SEC. Sudden and short-lived explosive events, such as the 29 September event, are common at Etna, and for such events, ash concentration is also low. On 16 November 2006, a very complex eruptive scenario

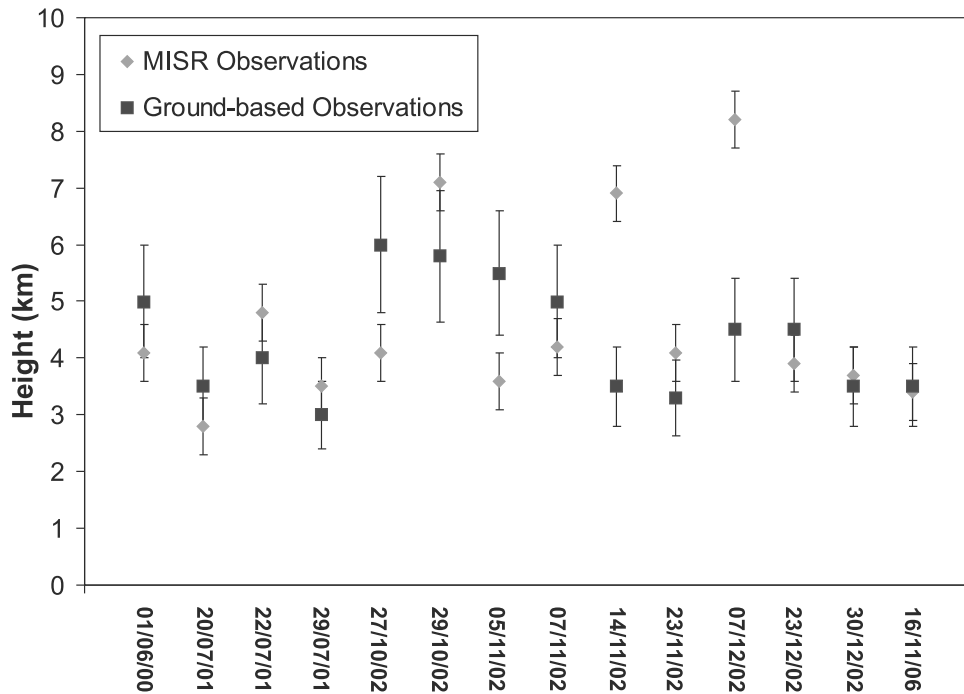


**Figure 5.** MISR wind-corrected heights compared with heights obtained by ground-based observations during the INGV-OE monitoring activities. Error bars for MISR observations are  $\pm 0.5$  km and error bars for ground-based observations are  $\pm 20\%$  of the column height.

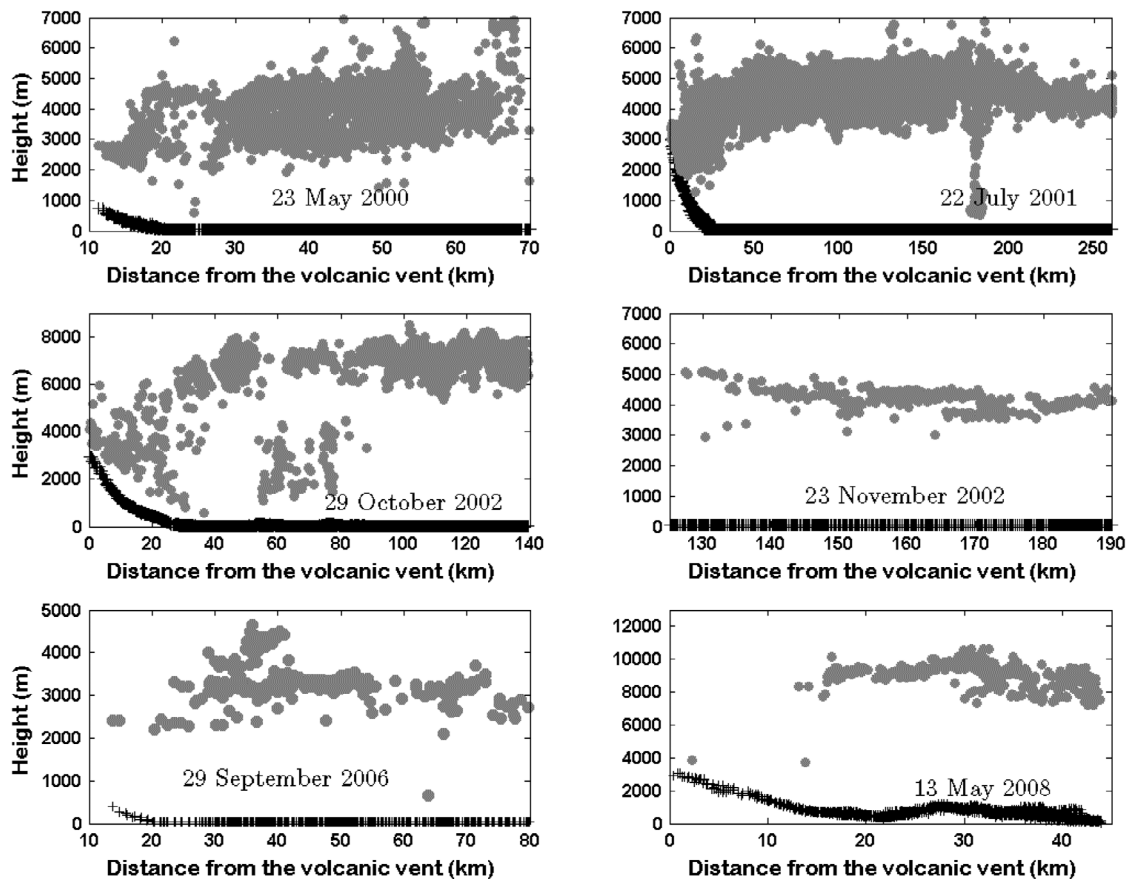


**Figure 6.** MISR wind-corrected heights as a function of the vent distance for some eruptive events. Gray points indicate MISR data; black crosses represent topography.

**Table 4.** Mean and Range of AOD Values, Mean and Range of MISR-Retrieved Green Band AOD Values Attributed to Spherical Particles, MISR-Retrieved Green-Band AOD Fraction of Particles Attributable to Small (<0.35  $\mu\text{m}$  Radius), Medium (Between 0.35 and 0.7  $\mu\text{m}$  Radius), and Large (>0.7  $\mu\text{m}$  Radius) Particle Sizes for Each of the Eruptive Events Obtained by the MINX Software<sup>a</sup>

Etna Eruption Time (UTC)	Mean AOD	AOD Range	AOD Sph. Fraction Mean	AOD Sph. Fract. Range	Small	Med	Large
<i>Ash-Dominated, Both MISR and Surface Observations: Mostly Large, Non-Spherical</i>							
27 Oct 2002 at 10:00 <sup>b</sup>	0.31	[0.04 0.58]	0.42	[0.1 1]	0.31	0.23	0.46
23 Dec 2002 at 09:54	0.11	[0.09 0.12]	0.43	[0.4 1]	0.40	0.11	0.49
30 Dec 2002 at 10:04 <sup>b</sup>	0.11	[0.04 0.14]	0.76	[0 1]	0.35	0.16	0.49
<i>Sulfate/Water-Dominated, Both MISR and Surface Observations: Mostly Small, Spherical</i>							
29 July 2001 at 10:01	0.18	[0.15 0.25]	0.93	[0.6 1]	0.77	0.09	0.13
23 Nov 2002 at 09:42 <sup>b</sup>	0.13	[0.07 0.19]	0.97	[0.2 1]	0.56	0.24	0.20
08 Jan 2003 at 09:54	0.15	[0.13 0.16]	0.95	[0.8 1]	0.49	0.08	0.43
29 Sept 2006 at 09:52	0.22	[0.15 0.26]	0.87	[0.6 1]	0.75	0.13	0.12
16 Nov 2006 at 09:46	0.08	[0.05 0.13]	0.94	[0.6 1]	0.67	0.08	0.25
25 Nov 2006 at 09:46	0.10	[0.05 0.15]	1	[1 1]	0.61	0.03	0.36
<i>Particle Type Surface Validation Data Lacking</i>							
23 May 2000 at 10:08 <sup>b</sup>	0.36	[0.26 0.38]	0.25	[0.2 0.4]	0.23	0.35	0.42
01 Jun 2000 at 10:02	0.14	[0.03 0.22]	0.89	[0.4 1]	0.72	0.15	0.13

<sup>a</sup>AOD Sph. Fraction Mean, mean MISR-retrieved green band AOD value attributed to spherical particles; AOD Sph. Fract. Range, range of MISR-retrieved green band AOD fraction attributed to spherical particles; Small, MISR-retrieved green-band AOD fraction of particles having small size (<0.35  $\mu\text{m}$  radius); Med, MISR-retrieved green-band AOD fraction of particles having medium size (0.35 < 0.7  $\mu\text{m}$  radius); and Large, MISR-retrieved green-band AOD fraction of particles having large size (>0.7  $\mu\text{m}$  radius).

<sup>b</sup>Volcanic ash detected by MODIS.

characterized by strombolian activity, lava effusion, emission of volcanic gases, avalanching episodes, minor collapses and propagation of eruptive fractures that formed a diluted plume, occurred during the MISR transit [Andronico *et al.*, 2009a]. Finally, for the 25 November 2006 case, MISR consistently retrieved aerosol containing only spherical components. This result is in agreement with field observations (Table 2) and NOAA–AVHRR polar satellite observations [Andronico *et al.*, 2009b].

[24] It should be noted that although all these cases had low AOD cases, which reduces confidence in the MISR aerosol retrievals [Kahn *et al.*, 2010], the aerosol type derived from MISR data was consistent in each case with those derived from near-coincident ground-based observations, obtained by reports, videos and photos taken by volcanologists during field surveys or from the automatic video-surveillance system.

[25] To further confirm our results, we analyzed the thermal infrared MODIS–Terra measurements from <http://ladsweb.nascom.nasa.gov/data/search.html>. In particular, for each eruptive event in Table 4, volcanic ash presence was verified using the Brightness Temperature Difference (BTD) technique [Wen and Rose, 1994]. We found that MODIS data of 23 May 2000, 27 October 2002, 23 November 2002, and 30 December 2002 all clearly show a volcanic ash plume (Figure 8) in agreement with MISR observations; the one exception is 23 December 2002, for which the cloudy weather conditions (Table 2) may have affected the retrieval. However, for this day, Andronico *et al.* [2008] reported an ash plume rising up to 4.5 km. Further supporting the MISR results, no volcanic ash was detected by the MODIS analysis for any of the sulphate and/or water vapor dominated plumes reported in Table 4, except for that of 23 November 2002. During this day, the first point retrieved by MISR, about 120 km from the volcanic vent, is within  $\sim 5$  km of the furthest downwind edge of the volcanic ash region as obtained by BTD (Figures 3 and 8). It is also possible that

during transit the fine ash components were altered, or mixed with background spherical aerosols and water vapor and/or sulphate components.

[26] MISR Standard aerosol retrieval results for the fraction of the green band AOD attributed to small (<0.35  $\mu\text{m}$ ), medium (between 0.35 and 0.7  $\mu\text{m}$ ), and large (>0.7  $\mu\text{m}$ ) particle sizes are also shown in Table 4. In all cases for which good observations were obtained, events identified as sulphate and/or water vapor-dominated have a larger fraction of fine components, whereas those identified based on particle shape as ash-dominated are characterized as having larger size particles.

#### 4. Discussion and Conclusion

[27] In this paper, we analyzed 20 volcanic plumes at Mt. Etna, Italy, between 2000 and 2008 using data from the Multiangle Imaging SpectroRadiometer. Plume height maps were derived from MISR multiangle, red-band observations using the MINX stereoscopic height retrieval tool. Aerosol amounts and types are derived, during standard processing, from MISR’s multiangle and multispectral observations. For each event, plume height and direction analyzed by MINX were compared with ground-based observations carried out by INGV-OE volcanologists during the monitoring of volcanic activity. The MISR Standard aerosol retrieval algorithm evaluates green-band AOD values, the green-band AOD fraction of spherical particles, and the green-band AOD fraction of particle size with a resolution of about three-to-five groupings (small, medium, large), allowing further investigation of the styles of explosive activity.

[28] Plume height is one of the most important input parameters for both volcanic ash dispersal modeling and retrievals. The total erupted mass (i.e., mass eruption rate multiplied by duration) is often obtained from eruption column estimates using inverse modeling [e.g., Folch *et al.*, 2008] or empirical relationships [e.g., Sparks *et al.*, 1997;

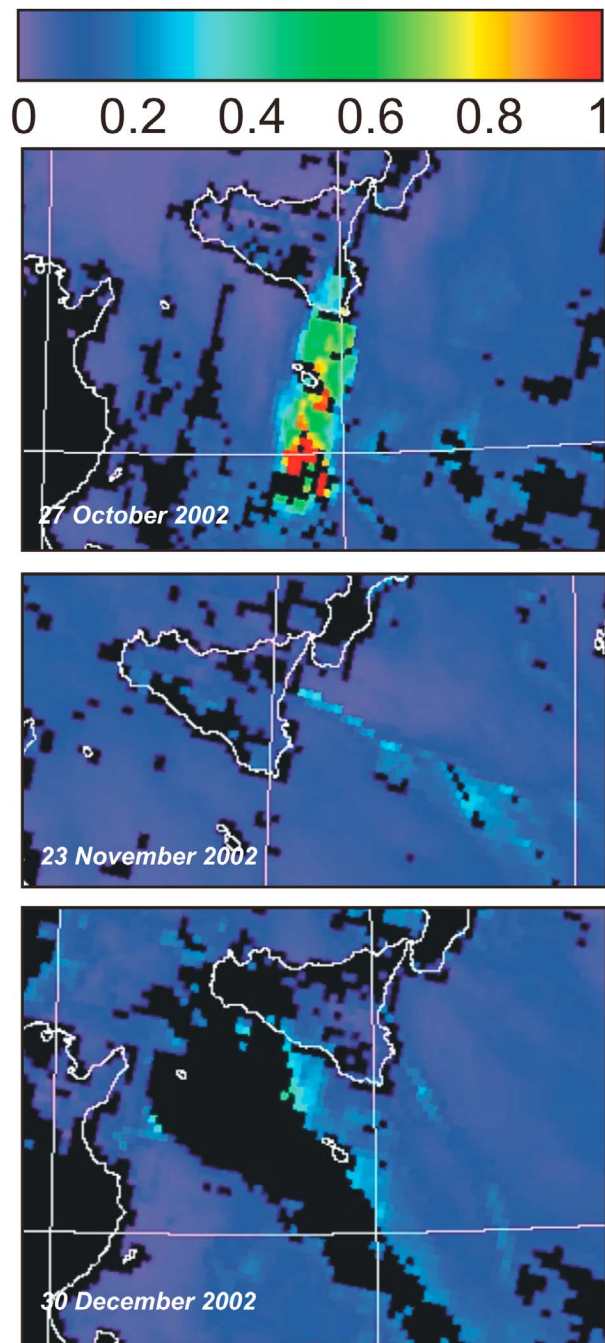


**Figure 7.** MODIS AOD images taken from <http://ladsweb.nascom.nasa.gov/data/search.html> at the same time as MISR transit for 27 October, 23 November, and 30 December 2002.

*Mastin*, 2009], which depend on accurate estimates of plume heights. *Tupper and Wunderman* [2009] note that the eruption column estimates from ground-based observations have several limitations that can produce up to 50% uncertainties. *Sparks et al.* [1997] recommend that ground-based observations should be made at a great distance from the volcanic vent. Cross-wind observations of the plume clearly distinguish the column height, whereas along-wind observations can underestimate the height. Furthermore, other issues, such as observer stress, partial or complete obscuring of the

volcanic plume (due for example to its own lateral spreading), and meteorological clouds may also affect plume top estimates. The estimation of cloud heights from MISR data has been widely validated in the past [*Naud et al.*, 2002, 2004, 2005]. We note that under good conditions (e.g., accurate user-supplied wind directions, high aerosol optical depths, largely horizontal aerosol motion) plume heights obtained using MISR data processed with the MINX tool can reach uncertainties  $< 0.5$  km. Furthermore, MISR data allow us to produce 2-D maps of plume-top heights over broad portions of a plume. Such maps are impossible to generate from isolated field observations.

[29] Etna produces a persistent degassing from summit craters, and pilots have reported the presence of volcanic ash in the gas plume during flight (Catania air traffic controllers, personal communication), even when there is no eruptive phase. In these cases, ash concentration is low, and is generally not dangerous to aircraft unless close to the volcano. As such, if MISR is used in combination with numerical models [e.g., *Scollo et al.*, 2010], it can furnish key information in cases when explosive activity produces volcanic ash plumes in concentrations that are hazardous to aviation. Furthermore, eruptive events having low amounts of ash cannot be easily quantified using traditional approaches, such as passive infrared methods [e.g., *Prata*, 1989]. For such eruptions the silicate signal can be too weak to overcome the effects of water vapor and instrument noise in split window algorithms [*Rose and Mayberry*, 2000]. We find that MISR can be used instead to map these plumes, and in future work, the results could be compared with those of more sophisticated split-window methods [e.g., *Yu et al.*, 2002; *Pavolonis*, 2010].

[30] Good agreement was found between MISR AOD retrievals and those obtained from a ground-based Sun photometer and from MODIS. As suggested by *Watson and Oppenheimer* [2001], systematic studies should be performed on active volcanoes such as Etna in order to validate and improve detections from satellite data. The permanent AERONET ([aeronet.gsfc.nasa.gov](http://aeronet.gsfc.nasa.gov)) Sun photometer station near the volcano can significantly improve our knowledge of Etna volcanic aerosols, and these measurements could be used to further test data obtained by MISR, as was successfully achieved in the case of desert dust [*Martonchik et al.*, 2004; *Kalashnikova and Kahn*, 2006].

[31] We find that differences in volcanic aerosol, produced by different eruptive styles, are recorded by MISR. In particular, an increase in the fraction of the green band AOD attributed to non-spherical particles is a good indicator of volcanic ash. This parameter can help to distinguish ash-dominated events from those dominated by sulphates and/or water vapor (e.g., spherical from non-spherical aerosol). This is an important feature from volcanological and atmospheric points of view. Changes in the physical state of volcanic emissions from gaseous into liquid phase can be detected in the MISR particle type retrievals under some circumstances. On the seven occasions when good quality and coincident MISR and ground-based observations were available, the MISR-retrieved aerosol was dominated by fine, mostly spherical particles (1 June 2000, 29 July 2001, 23 November 2002, 8 January 2003, 29 September 2006, 16 and 25 November 2006) indicating sulphate or/and water dominated plumes. For

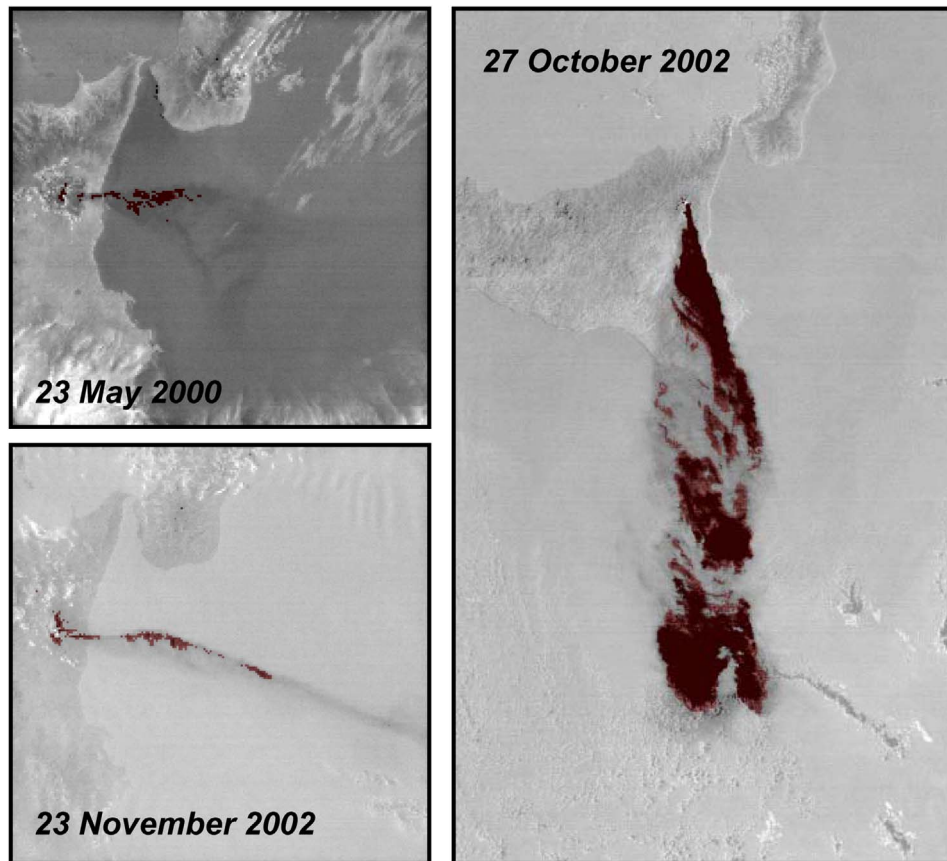


**Figure 8.** MODIS images of 23 May 2000 (1005 UTC), 27 October 2002 (1000 UTC) and 23 November 2002 (0945 UTC) taken from <http://ladsweb.nascom.nasa.gov/data/search.html>. Black color plume indicates volcanic ash retrieved using the BTM technique.

these events, the MODIS analysis using the BTM technique does not show the presence of volcanic ash in the region retrieved by MISR. In addition, non-ash (sulphate and water vapor) and ash particles constitute two different particle size modes, as natural ash particle size distributions tend to be coarse-mode dominated, whereas sulphate particles tend to be fine-mode dominated [Ansmann *et al.*, 2011]; we find this pattern to be reproduced consistently in our analysis of the MISR observations. The presence of coarse-mode particles such as volcanic ash can affect cloud properties, hence modifying the impact volcanic plumes have on the atmosphere. In fact, ash particles are favorable ice nuclei and consequently may support ice formation [Durant *et al.*, 2008]. Furthermore, our results show that good MISR aerosol retrievals were obtained for eleven of twelve events analyzed in this paper. Upgrades to the MISR Version 22 aerosol retrieval algorithm, such as improved component and mixture options in the algorithm climatology, and increased retrieval product spatial resolution (17.6 km in the current version), could better identify the presence of volcanic aerosols, thereby improving MISR's capabilities for this application [e.g., Kahn *et al.*, 2010].

[32] In conclusion, plume height and direction derived from MISR data for twenty eruptive events of Mt. Etna were in good agreement with ground-based observations. In the case of plume height, MISR observations are more

comprehensive than measurements obtained by isolated ground-based observations. Consequently, MISR plume heights can be used as inputs for volcanic ash dispersal models and retrieval procedures in order to improve both the plume dispersal prediction and quantitative ash retrievals. MISR data clearly detected the presence of volcanic ash even when the concentration was low. The particle type parameter seems to reflect the style of the explosive activity, consistently distinguishing ash-dominated from sulphate/water vapor dominated plumes. We find that sulphate/water vapor dominated plumes are characterized by particles having a smaller size than particles in ash-dominated plumes. Hence, we conclude that MISR data, collected globally for more than 12 years, since late February 2000, furnishes new information on volcanic activity and can contribute significantly to our understanding of the atmospheric impact of volcanic plumes, and in particular, to the explosive volcanism of active volcanoes such as Etna.

[33] **Acknowledgments.** The MISR data used in this study were obtained from the NASA Langley Research Center Atmospheric Science Data Center. Volcanological information was obtained by INGV-OE reports of Etna activity. The authors thank Boris Behncke, who furnished information of the 2000 Etna activity, three anonymous reviewers who greatly improved the quality of the paper, and the native speaker Stephen Conwey. This work was partially funded by the FIRB project "Sviluppo Nuove Tecnologie per la Protezione e Difesa del Territorio dai Rischi Naturali" of Italian Ministry of Universities and Research for one of the authors (S. Scollo). Part of this research was performed at the Jet Propulsion

Laboratory, California Institute of Technology, under a contract with the National Aeronautics and Space Administration. The work of R. Kahn is supported in part by NASA's Climate and Radiation Research and Analysis Program, under H. Maring, NASA's Atmospheric Composition Program, and the EOS-MISR project.

## References

- Alparone, S., D. Andronico, L. Lodato, and T. Sgroi (2003), Relationship between tremor and volcanic activity during the Southeast Crater eruption on Mount Etna in early 2000, *J. Geophys. Res.*, *108*(B5), 2241, doi:10.1029/2002JB001866.
- Alparone, S., D. Andronico, T. Sgroi, F. Ferrari, L. Lodato, and D. Reitano (2007), Alert system to mitigate tephra fallout hazards at Mt Etna volcano, Italy, *Nat. Hazards*, *43*, 333–350, doi:10.1007/s11069-007-9120-7.
- Andronico, D., et al. (2005), A multi-disciplinary study of the 2002–03 Etna eruption: Insights for a complex plumbing system, *Bull. Volcanol.*, *67*(4), 314–330, doi:10.1007/s00445-004-0372-8.
- Andronico, D., S. Scollo, A. Cristaldi, and S. Caruso (2008), The 2002–2003 Etna explosive activity: Tephra dispersal and features of the deposit, *J. Geophys. Res.*, *113*, B04209, doi:10.1029/2007JB005126.
- Andronico, D., S. Scollo, A. Cristaldi, and F. Ferruccio (2009a), Monitoring ash emission episodes at Mt. Etna: The 16 November 2006 case study, *J. Volcanol. Geotherm. Res.*, *180*, 123–134, doi:10.1016/j.jvolgeores.2008.10.019.
- Andronico, D., C. Spinetti, A. Cristaldi, and M. F. Buongiorno (2009b), Observations of Mt. Etna volcanic ash plumes in 2006: An integrated approach from ground-based and polar satellite NOAA–AVHRR monitoring system, *J. Volcanol. Geotherm. Res.*, *180*, 135–147, doi:10.1016/j.jvolgeores.2008.11.013.
- Ansmann A., et al. (2011), Ash and fine-mode particle mass profiles from EARLINET–AERONET observations over central Europe after the eruptions of the Eyjafjallajökull volcano in 2010, *J. Geophys. Res.*, *116*, D00U02, doi:10.1029/2010JD015567.
- Barsotti, S., D. Andronico, A. Neri, P. Del Carlo, P. J. Baxter, W. P. Aspinall, and T. Hincks (2010), Quantitative assessment of volcanic ash hazards for health and infrastructure at Mt. Etna (Italy) by numerical simulation, *J. Volcanol. Geotherm. Res.*, *192*(1–2), 85–96, doi:10.1016/j.jvolgeores.2010.02.011.
- Behncke, B., M. Neri, E. Pecora, and V. Zanon (2006), The exceptional activity and growth of the Southeast Crater, Mount Etna (Italy), between 1996 and 2001, *Bull. Volcanol.*, *69*, 149–173, doi:10.1007/s00445-006-0061-x.
- Behncke, B., S. Falsaperla, and E. Pecora (2009), Complex magma dynamics at Mount Etna revealed by seismic, thermal, and volcanological data, *J. Geophys. Res.*, *114*, B03211, doi:10.1029/2008JB005882.
- Bonaccorso, A., A. Bonforte, S. Calvari, C. Del Negro, G. Di Grazia, G. Ganci, M. Neri, A. Vicari, and E. Boschi (2011), The initial phases of the 2008–2009 Mount Etna eruption: A multidisciplinary approach for hazard assessment, *J. Geophys. Res.*, *116*, B03203, doi:10.1029/2010JB007906.
- Calvari, S., and H. Pinkerton (2004), Birth, growth and morphologic cinder cone during the evolution of the ‘Laghetto’ 2001 Etna eruption, *J. Volcanol. Geotherm. Res.*, *132*, 225–239, doi:10.1016/S0377-0273(03)00347-0.
- Calvari, S., et al. (2001), Multidisciplinary approach yields insight into Mt. Etna 2001 eruption, *Eos Trans. AGU*, *82*(52), 653–656, doi:10.1029/01EO00376.
- Corradini, S., C. Spinetti, E. Carboni, C. Tirelli, M. F. Buongiorno, S. Pugnaghi, and G. Gangale (2008), Mt. Etna tropospheric ash retrieval and sensitivity analysis using Moderate Resolution Imaging Spectroradiometer measurements, *J. Appl. Remote Sens.*, *2*, 023550, doi:10.1117/1.3046674.
- Corradini, S., L. Merucci, and A. J. Prata (2009), Retrieval of SO<sub>2</sub> from thermal infrared satellite measurements: Correction procedures for the effects of volcanic ash, *Atmos. Meas. Techniques*, *2*, 177–191, doi:10.5194/amt-2-177-2009.
- Corradini, S., L. Merucci, and A. Folch (2011), Volcanic ash cloud properties: Comparison between MODIS satellite retrievals and FALL3D transport model, *IEEE Trans. Geosci. Remote Sens.*, *8*, 248–252, doi:10.1109/LGRS.2010.2064156.
- Diner, D. J., et al. (1998), Multiangle Imaging Spectroradiometer (MISR) instrument description and experiment overview, *IEEE Trans. Geosci. Remote Sens.*, *36*, 1072–1087, doi:10.1109/36.700992.
- Durant, A. J., R. A. Shaw, W. I. Rose, Y. Mi and G. G. J. Ernst (2008), Ice nucleation and over seeding of ice in volcanic clouds, *J. Geophys. Res.*, *113*, D09206, doi:10.1029/2007JD009064.
- Folch, A., O. Jorba, and J. Viramonte (2008), Volcanic ash forecast—Application to the May 2008 Chaiten eruption, *Nat. Hazards Earth Syst. Sci.*, *94*, 109–117.
- Fromm, M., O. Torres, D. Diner, D. Lindsey, B. V. Hull, R. Servranckx, E. P. Shettle, and Z. Li (2008), Stratospheric impact of the Chisholm pyroclumulonimbus eruption: 1. Earth-viewing satellite perspective, *J. Geophys. Res.*, *113*, D08202, doi:10.1029/2007JD009153.
- Kahn, R. A., W. H. Li, C. Moroney, D. J. Diner, J. V. Martonchik, and E. Fishbein (2007), Aerosol source plume physical characteristics from space-based multiangle imaging, *J. Geophys. Res.*, *112*, D11205, doi:10.1029/2006JD007647.
- Kahn, R. A., B. J. Gaitley, M. J. Garay, D. J. Diner, T. Eck, A. Smirnov, and B. N. Holben (2010), Multiangle Imaging Spectroradiometer global aerosol product assessment by comparison with the Aerosol Robotic Network, *J. Geophys. Res.*, *115*, D23209, doi:10.1029/2010JD014601.
- Kalashnikova, O. V., and R. Kahn (2006), Ability of multiangle remote sensing observations to identify and distinguish mineral dust types: 2. Sensitivity over dark water, *J. Geophys. Res.*, *111*, D11207, doi:10.1029/2005JD006756.
- Marchand, R., T. Ackerman, M. Smyth, and W. B. Rossow (2010), A review of cloud top height and optical depth histograms from MISR, ISCCP, and MODIS, *J. Geophys. Res.*, *115*, D16206, doi:10.1029/2009JD013422.
- Martonchik, J. V., D. J. Diner, R. Kahn, B. Gaitley, and B. N. Holben (2004), Comparison of MISR and AERONET aerosol optical depths over desert sites, *Geophys. Res. Lett.*, *31*, L16102, doi:10.1029/2004GL019807.
- Martonchik, J. V., R. A. Kahn, and D. J. Diner (2009), Retrieval of aerosol properties over land using MISR observations, in *Satellite Aerosol Remote Sensing Over Land*, edited by A. A. Kokhanovsky and G. de Leeuw, pp. 267–293, Springer, Berlin, doi:10.1007/978-3-540-69397-0\_9.
- Mastin, L. G. (2009), A user-friendly one-dimensional model for wet volcanic plumes, *Geochem. Geophys. Geosyst.*, *8*, Q03014, doi:10.1029/2006GC001455.
- Moroney, C., R. Davies, and J. Muller (2002), Operational retrieval of cloud-top heights using MISR data, *IEEE Trans. Geosci. Remote Sens.*, *40*, 1532–1540, doi:10.1109/TGRS.2002.801150.
- Muller, J. P., A. Mandanayake, C. Moroney, R. Davies, D. J. Diner, and S. Paradise (2002), MISR stereoscopic image matchers: Techniques and results, *IEEE Trans. Geosci. Remote Sens.*, *40*, 1547–1559, doi:10.1109/TGRS.2002.801160.
- Naud, C., J. P. Muller, and E. E. Clothiaux (2002), Comparison of cloud top heights derived from MISR stereo and MODIS CO<sub>2</sub>-slicing, *Geophys. Res. Lett.*, *29*(16), 1795, doi:10.1029/2002GL015460.
- Naud, C., J. Muller, M. Haeffelin, Y. Morille, and A. Delaval (2004), Assessment of MISR and MODIS cloud top heights through inter-comparison with a back-scattering lidar at SIRTa, *Geophys. Res. Lett.*, *31*, L04114, doi:10.1029/2003GL018976.
- Naud, C. M., J.-P. Muller, E. E. Clothiaux, B. A. Baum, and W. P. Menzel (2005), Intercomparison of multiple years of MODIS, MISR and radar cloud-top heights, *Ann. Geophys.*, *23*, 2415–2424, doi:10.5194/angeo-23-2415-2005.
- Nelson, D. L., Y. Chen, R. A. Kahn, D. J. Diner, and D. Mazzoni (2008), Example applications of the MISR Interactive eXplorer (MINX) software tool to wildfire smoke plume applications, *Proc. SPIE Int. Soc. Opt. Eng.*, *7089*, 708908.
- Neri, M., B. Behncke, M. Burton, G. Galli, S. Giammanco, E. Pecora, E. Privitera, and D. Reitano (2006), Continuous soil radon monitoring during the July 2006 Etna eruption, *Geophys. Res. Lett.*, *33*, L24316, doi:10.1029/2006GL028394.
- Norini, G., E. De Beni, D. Andronico, M. Polacci, M. Burton, and F. Zucca (2009), The 16 November 2006 flank collapse of South-East Crater at Mount Etna, Italy: Study of the deposit and hazard assessment, *J. Geophys. Res.*, *114*, B02204, doi:10.1029/2008JB005779.
- Pavolonis, M. J. (2010), Advances in extracting cloud composition information from spaceborne infrared radiances: A robust alternative to brightness temperatures. Part I: Theory, *J. Appl. Meteorol. Climatol.*, *49*, 1992–2012, doi:10.1175/2010JAMC2433.1.
- Prata, A. J. (1989), Observations of volcanic ash clouds in the 10–12-micron window using AVHRR/2 data, *Int. J. Remote Sens.*, *10*, 751–761, doi:10.1080/01431168908903916.
- Pugnaghi, S., G. Gangale, S. Corradini, and M. F. Buongiorno (2006), Mt. Etna sulphur dioxide flux monitoring using ASTER-TIR data and atmospheric observations, *J. Volcanol. Geotherm. Res.*, *152*, 74–90, doi:10.1016/j.jvolgeores.2005.10.004.
- Rose, W. I., and G. C. Mayberry (2000), Use of GOES thermal infrared imagery for eruption scale measurements, Soufrière Hills, Montserrat, *Geophys. Res. Lett.*, *27*, 3097–3100, doi:10.1029/1999GL008459.
- Scollo, S. (2006), Study of fallout processes of volcanic particles from explosive Etna eruptions, PhD alma mater studiorum, Univ. di Bologna, Bologna, Italy.

- Scollo, S., P. Del Carlo, and M. Coltelli (2007), Tephra fallout of 2001 Etna flank eruption: Analysis of the deposit and plume dispersion, *J. Volcanol. Geotherm. Res.*, *160*, 147–164, doi:10.1016/j.jvolgeores.2006.09.007.
- Scollo, S., A. Folch, and A. Costa (2008), A parametric and comparative study on different tephra fallout models, *J. Volcanol. Geotherm. Res.*, *176*, 199–211, doi:10.1016/j.jvolgeores.2008.04.002.
- Scollo, S., M. Prestifilippo, G. Spata, M. D'Agostino, and M. Coltelli (2009), Forecasting and monitoring Etna volcanic plumes, *Nat. Hazards Earth Syst. Sci.*, *9*, 1573–1585, doi:10.5194/nhess-9-1573-2009.
- Scollo, S., A. Folch, M. Coltelli, and V. J. Realmuto (2010), Three-dimensional volcanic aerosol dispersal: A comparison between Multiangle Imaging Spectroradiometer (MISR) data and numerical simulations, *J. Geophys. Res.*, *115*, D24210, doi:10.1029/2009JD013162.
- Sparks, R. S. J., M. I. Bursik, S. N. Carey, J. S. Gilbert, L. S. Glaze, H. Sigurdsson, and A. W. Woods (1997), Observations and interpretation of volcanic plumes, in *Volcanic Plumes*, pp. 117–140, John Wiley, Chichester, U. K.
- Stenchikov, G., N. Lahoti, P. J. Liroy, P. G. Georgopoulos, D. J. Diner, and R. Kahn (2006), Multiscale plume transport from collapse of the World Trade Center on September 11, 2001, *Environ. Fluid Mech.*, *6*, 425–450, doi:10.1007/s10652-006-9001-8.
- Taddeucci, J., M. Pompilio, and P. Scarlato (2002), Monitoring the explosive activity of the July–August 2001 eruption of Mt Etna (Italy) by ash characterization, *Geophys. Res. Lett.*, *29*(8), 1230, doi:10.1029/2001GL014372.
- Tosca, M. G., J. T. Randerson, C. S. Zender, D. L. Nelson, D. J. Diner, and J. A. Logan (2011), Dynamics of fire plumes and smoke clouds associated with peat and deforestation fires in Indonesia, *J. Geophys. Res.*, *116*, D08207, doi:10.1029/2010JD015148.
- Tupper, A., and R. Wunderman (2009), Reducing discrepancies in ground and satellite-observed eruption heights, *J. Volcanol. Geotherm. Res.*, *186*, 22–31, doi:10.1016/j.jvolgeores.2009.02.015.
- Val Martin, M. V., J. A. Logan, R. A. Kahn, F. Y. Leung, D. L. Nelson, and D. J. Diner (2010), Smoke injection heights from fires in North America: Analysis of 5 years of satellite observations, *Atmos. Chem. Phys.*, *10*, 1491–1510, doi:10.5194/acp-10-1491-2010.
- Watson, I. M., and C. Oppenheimer (2001), Photometric observations of Mt. Etna's different aerosol plumes, *Atmos. Environ.*, *35*, 3561–3572, doi:10.1016/S1352-2310(01)00075-9.
- Wen, S., and W. I. Rose (1994), Retrieval of sizes and total masses of particles in volcanic clouds using AVHRR bands 4 and 5, *J. Geophys. Res.*, *99*, 5421–5431, doi:10.1029/93JD03340.
- Yu, T. X., W. I. Rose, and A. J. Prata (2002), Atmospheric correction for satellite-based volcanic ash mapping and retrievals using “split window” IR data from GOES and AVHRR, *J. Geophys. Res.*, *107*(D16), 4311, doi:10.1029/2001JD000706.

---

M. Coltelli and S. Scollo, Istituto Nazionale di Geofisica e Vulcanologia, Osservatorio Etno, Sezione di Catania, Piazza Roma 2, I-95125 Catania, Italy. (simona.scollo@ct.ingv.it)

D. J. Diner, M. J. Garay, and V. J. Realmuto, Jet Propulsion Laboratory, California Institute of Technology, Pasadena, CA 91109, USA.

R. A. Kahn, Atmospheres Laboratory, NASA Goddard Space Flight Center, Greenbelt, MD 20771, USA.

D. L. Nelson, Raytheon Company, Pasadena, CA 91101, USA.